symmetry

MDPI

*Article*

# Ferromagnet-Type System: Integrable Flows of Curves/Surfaces, Soliton Solutions, and Equivalence

**Gulgassyl Nugmanova [1], Guldana Bekova [2,*], Meruyert Zhassybayeva [2,*], Aigul Taishiyeva [3], Kuralay Yesmakhanova [1] and Zhaidary Myrzakulova [4]**

[1] Department of Mathematical and Computer Modeling, L.N. Gumilyov Eurasian National University, Astana 010000, Kazakhstan; kryesmakhanova@gmail.com (K.Y.)
[2] Department of General and Theoretical Physics, L.N. Gumilyov Eurasian National University, Astana 010000, Kazakhstan
[3] Department of Mathematics and Methods of Teaching Mathematics, Kh. Dosmukhamedov Atyrau University, Atyrau 060000, Kazakhstan
[4] Department of Algebra and Geometry, L.N. Gumilyov Eurasian National University, Astana 010000, Kazakhstan
* Correspondence: bekovaguldana@gmail.com (G.B.); mbzhassybayeva@gmail.com (M.Z.)

**Abstract**

This paper investigates an integrable spin system known as the Myrzakulov-XIII (M-XIII) equation through geometric and gauge-theoretic methods. The M-XIII equation, which describes dispersionless dynamics with curvature-induced interactions, is shown to admit a geometric interpretation via curve flows in three-dimensional space. We establish its gauge equivalence with the complex coupled dispersionless (CCD) system and construct the corresponding Lax pair. Using the Sym–Tafel formula, we derive exact soliton surfaces associated with the integrable evolution of curves and surfaces. A key focus is placed on the role of geometric and gauge symmetry in the integrability structure and solution construction. The main contributions of this work include: (i) a commutative diagram illustrating the connections between the M-XIII, CCD, and surface deformation models; (ii) the derivation of new exact solutions for a fractional extension of the M-XIII equation using the Kudryashov method; and (iii) the classification of these solutions into trigonometric, hyperbolic, and exponential types. These findings deepen the interplay between symmetry, geometry, and soliton theory in nonlinear spin systems.

**Keywords:** ferromagnet-type system; integrable flows of curves/surfaces; gauge equivalent; fractional CCD equation; soliton solution



Academic Editor: Calogero Vetro

Received: 27 May 2025
Revised: 20 June 2025
Accepted: 24 June 2025
Published: 2 July 2025

**Citation:** Nugmanova, G.; Bekova, G.; Zhassybayeva, M.; Taishiyeva, A.; Yesmakhanova, K.; Myrzakulova, Z. Ferromagnet-Type System: Integrable Flows of Curves/Surfaces, Soliton Solutions, and Equivalence. *Symmetry* **2025**, *17*, 1041. https://doi.org/10.3390/sym17071041



## 1. Introduction

The study of integrable nonlinear equations has long served as a cornerstone in mathematical physics, with profound connections to geometry, field theory, and the modeling of complex physical phenomena. Among the most prominent examples is the classical Heisenberg ferromagnet (HF) equation [1–3]

$$iA_t + \frac{1}{2}[A, A_{xx}] = 0, \tag{1}$$

which models spin wave dynamics in ferromagnetic materials and admits a Lax pair formulation [4], allowing its exact solvability via the inverse scattering transform [5]. The equation belongs to the broader class of integrable spin systems and nonlinear dynamical models that

describe the evolution of spin fields in one or more spatial dimensions. These models not only possess rich mathematical structures but also have direct relevance to physical systems such as magnetic chains, nematic liquid crystals, spintronics, and Bose–Einstein condensates, where soliton-like excitations and spin dynamics play a crucial role in describing quantum coherence and nonlinear wave propagation [6,7].

Soliton theory has emerged as a particularly powerful framework for understanding the nonlinear dynamics of such systems. Solitons are localized stable wave packets that arise in a wide variety of integrable models, ranging from the Korteweg–de Vries (KdV) [8] and sine–Gordon equations [9] to nonlinear Schrödinger-type and derivative equations [10,11]. Their remarkable stability under interaction along with their geometric manifestations have led to deep exploration of soliton equations through differential geometry, Hamiltonian structures [12,13], and gauge theories [14,15].

In the context of integrable spin systems, soliton solutions often describe topologically stable configurations such as spin waves, breathers, and magnetic domain walls. A range of analytical techniques—including inverse scattering [16], Darboux transformations [17,18], and bilinear methods [19]—have been employed to construct such solutions, providing insights into both mathematical structure and physical behavior.

Over the years, numerous generalizations and multidimensional extensions of the HF equation have been proposed to capture more intricate spin interactions, geometric effects, and physical constraints [20–22]. Notably, the Landau–Lifshitz equation, the Ishimori equation, and the Lakshmanan–Myrzakulov-type equations have been studied extensively [23,24]. These models introduce higher-order effects, anisotropies, and multidimensional geometrical interpretations, revealing deep interconnections between soliton equations and the motion of curves and surfaces embedded in $\mathbb{R}^3$ [25,26].

A particularly influential line of research has addressed the geometric interpretation of integrable equations as Hamiltonian flows of curves and surfaces, a direction developed by Anco and Myrzakulov [27] as well as by Myrzakulov et al. [28,29], who investigated integrable Heisenberg ferromagnets and soliton geometry of curves and surfaces. In their work, they demonstrated that integrable spin systems and Schrödinger maps can be understood as arising from geometric curve flows governed by moving frame equations [30]. Through the use of differential invariants and bi-Hamiltonian structures [31,32], this approach unifies many known models—including the Heisenberg and mKdV spin chains—under a broader geometric framework. Moreover, they introduced integrable surface deformations [29,33], extending the theory to (2+1)-dimensions and establishing deep links between soliton theory, surface geometry, and gauge equivalence. In parallel, the asymptotic equivalence between integrable shallow water wave models such as the Camassa–Holm and fifth-order KdV equations has been demonstrated using nonlinear and nonlocal transformations [34]. Building upon previous studies by Anco and Myrzakulov [27–29] which explored the geometric evolution of curves and surfaces in integrable spin systems, the present work extends the framework to the fractional M-XIII model and provides explicit soliton surface constructions.

In particular, integrable spin systems have been shown to admit geometrical interpretations in terms of the motion of space curves and surfaces, where curvature and torsion encode the dynamical evolution of the spin fields. The use of moving frames, differential invariants, and gauge connections has further enriched this interplay between geometry and soliton theory.

One notable generalization is the Myrzakulov-XIII (M-XIII) equation, which arises in the context of integrable flows of curves and surfaces. This model features dispersionless dynamics and curvature-induced interactions, making it a valuable candidate for exploring the interplay between geometry and soliton theory. The M-XIII equation can be viewed as

an integrable deformation of the HF equation that preserves its geometric richness while introducing new structures.

In this work, we undertake a detailed investigation of the M-XIII equation from both a geometric and gauge-theoretic perspective. We demonstrate that the M-XIII equation is geometrically equivalent to the complex coupled dispersionless (CCD) equation, which describes integrable evolution of curvature-modulated complex fields. Moreover, we construct the Lax pair of the M-XIII equation and establish its gauge equivalence with the CCD system via an explicit transformation.

Furthermore, we analyze the integrable curve and surface flows generated by the M-XIII equation by considering two distinct identifications of the spin field with geometric quantities. In each case, we derive the associated Frenet–Serret frame, Gauss–Weingarten equations, and soliton surfaces, leading to exact analytical solutions via the Sym–Tafel formula.

In recent years, increasing attention has been directed toward fractional and variable-coefficient generalizations of integrable nonlinear models. These fractional partial differential equations (FPDEs) incorporate derivatives of non-integer order, providing accurate descriptions of memory effects and nonlocality in physical systems such as optical media, magnetic chains, and viscoelastic materials. Extensions of inverse scattering techniques and analytical methods have led to exact soliton, breather, and periodic solutions for generalized models, including fractional nonlinear Schrödinger, Hirota–Maccari, and Fokas–Lenells equations [35–37]. Motivated by these developments, the present work investigates a fractional deformation of the M-XIII equation and constructs new classes of exact solutions using the Kudryashov method. The results not only enrich the solution space of classical models but also open up new avenues for analyzing curvature-induced phenomena, gauge equivalence, and the geometry of integrable flows under fractional dynamics.

Building on these fractional developments, our results reveal the deep structural connections between integrable spin models and differential geometry while opening pathways to new applications in mathematical physics, including nonlinear optics, low-dimensional magnetism, and geometry-induced soliton phenomena [38–44].

## 2. The Myrzakulov-XIII Equation

In this section, we consider the integrable Myrzakulov-XIII (M-XIII) equation, which represents a (2+1)-dimensional generalization of classical spin models. This equation describes the evolution of a spin field, which is expressed as a Hermitian $2 \times 2$ matrix of unit norm and which can be interpreted as a spin vector constrained by $A^2 = I$. The M-XIII model is particularly notable for its dispersionless nature and curvature-induced interactions, making it highly relevant in the study of geometric spin systems.

The M-XIII equation is written as follows:

$$iA_t = \frac{1}{2k}[A, A_t]_x + \frac{i}{k^2}(\rho A)_x \tag{2}$$

where $A$ is the spin matrix, $k$ is a real constant, and $\rho$ is a scalar function incorporating geometric effects. The scalar function $\rho$ is provided by

$$\rho = \sqrt{1 - \frac{\sigma k^2}{2} tr(A_t^2)} = \sqrt{1 - \sigma k^2 \mathbf{A}_t^2}, \quad \mathbf{A} = (A_1, A_2, A_3), \quad \mathbf{A}^2 = 1$$

and plays a role analogous to curvature-induced modulation in the dynamics of the spin field. The spin matrix satisfies the constraint $A^2 = I$ and is parameterized in terms of Pauli matrices as follows:

$$A = \begin{pmatrix} A_3 & \sigma A^- \\ A^+ & -A_3 \end{pmatrix}, \quad A^\pm = A_1 \pm iA_2$$

with the normalization condition

$$\sigma(A_1^2 + A_2^2) + A_3^2 = 1,$$

where $\sigma = \pm 1$ determines the type of geometry. Here, $\sigma = +1$ corresponds to the elliptic (spherical) case and $\sigma = -1$ to the hyperbolic case.

The integrability of the M-XIII equation is confirmed by the existence of a Lax pair

$$\Phi_x = i(k-\lambda)A\Phi = U_1\Phi, \tag{3}$$

$$\Phi_t = \left[\frac{i(k-\lambda)}{4k\lambda}\rho A + \frac{(k-\lambda)}{2\lambda}AA_t\right]\Phi = V_1\Phi, \tag{4}$$

where $\Phi$ is an eigenfunction and $\lambda$ is the spectral parameter. This pair ensures that the compatibility condition leads back to the M-XIII equation, making it part of the class of integrable systems.

Physically, the M-XIII equation can be interpreted as describing spin dynamics constrained by geometric quantities such as curvature and torsion. This makes it relevant for modeling nonlinear excitations in magnetically ordered materials as well as in geometric contexts such as the evolution of space curves, which we explore in the following sections.

## 3. Integrable Flows of Space Curves Induced by the M-XIII Equation

Let us now derive the Lakshmanan-type (geometrical) equivalent form of the M-XIII Equation (2) for the case $\sigma = 1$. To do this, we rewrite the the M-XIII equation in vector form. Several equivalent vector representations are available:

Form I:

$$\mathbf{A}_t = \frac{1}{k}(\mathbf{A} \wedge \mathbf{A}_t)_x + \frac{1}{k^2}(\rho\mathbf{A})_x, \tag{5}$$

$$\rho_x = k\mathbf{A} \cdot (\mathbf{A}_t \wedge \mathbf{A}_x) \tag{6}$$

Form II:

$$\mathbf{A}_t = \frac{1}{k}\mathbf{A} \wedge \mathbf{A}_{xt} + \frac{1}{k^2}\rho\mathbf{A}_x, \tag{7}$$

$$\rho_x = k\mathbf{A} \cdot (\mathbf{A}_t \wedge \mathbf{A}_x) \tag{8}$$

Form III:

$$\mathbf{A}_t = \frac{1}{k}\mathbf{A} \wedge \mathbf{A}_{xt} + \frac{1}{k}\partial_x^{-1}[\mathbf{A} \cdot (\mathbf{A}_t \wedge \mathbf{A}_x)]\mathbf{A} \tag{9}$$

Form IV:

$$\mathbf{A}_t = \frac{1}{k}\mathbf{A} \wedge \mathbf{A}_{xt} \pm \frac{1}{k^2}\sqrt{1 - \sigma k^2\,\mathbf{A}_t^2}\mathbf{A}_x. \tag{10}$$

Now, we consider a space curve in $\mathbb{R}^3$ defined by a set orthonormal vectors $\mathbf{l}_k$. These vectors satisfy the Frenet–Serret equations:

$$\begin{pmatrix} \mathbf{l}_1 \\ \mathbf{l}_2 \\ \mathbf{l}_3 \end{pmatrix}_x = C \begin{pmatrix} \mathbf{l}_1 \\ \mathbf{l}_2 \\ \mathbf{l}_3 \end{pmatrix}, \quad \begin{pmatrix} \mathbf{l}_1 \\ \mathbf{l}_2 \\ \mathbf{l}_3 \end{pmatrix}_t = G \begin{pmatrix} \mathbf{l}_1 \\ \mathbf{l}_2 \\ \mathbf{l}_3 \end{pmatrix}$$

where $\mathbf{l}_1, \mathbf{l}_2, \mathbf{l}_3$ are the tangent, normal, and binormal unit vectors, respectively. The matrices $C$ and $G$ have the forms

$$C = \begin{pmatrix} 0 & \kappa & 0 \\ -\kappa & 0 & \tau \\ 0 & -\tau & 0 \end{pmatrix}, \quad G = \begin{pmatrix} 0 & \gamma_3 & -\gamma_2 \\ -\gamma_3 & 0 & \gamma_1 \\ \gamma_2 & -\gamma_1 & 0 \end{pmatrix},$$

where $\kappa$ and $\tau$ denote the curvature and torsion of the curve, respectively, which are defined by

$$\kappa = \sqrt{\mathbf{l}_{1x}^2}, \quad \tau = \frac{\mathbf{l}_1 \cdot (\mathbf{l}_{1x} \wedge \mathbf{l}_{1xx})}{\mathbf{l}_{1x}^2}. \tag{11}$$

The compatibility condition of the Frenet–Serret system yields

$$C_t - G_x + [C, G] = 0, \tag{12}$$

which results in the following evolution equations:

$$\kappa_t = \gamma_{3x} + \tau\gamma_2, \tag{13}$$
$$\tau_t = \gamma_{1x} - \kappa\gamma_2, \tag{14}$$
$$\gamma_{2x} = \tau\gamma_3 - \kappa\gamma_1. \tag{15}$$

Now, we perform the following identification:

$$\mathbf{A} \equiv \mathbf{l}_1. \tag{16}$$

Then, from this identification, the following relations hold:

$$\kappa^2 = \mathbf{A}_x^2, \tag{17}$$
$$\tau = \frac{\mathbf{A} \cdot (\mathbf{A}_x \wedge \mathbf{A}_{xx})}{\mathbf{A}_x^2}. \tag{18}$$

The coefficients $\gamma_1$, $\gamma_2$, $\gamma_3$ can be expressed as

$$\gamma_1 = \frac{\kappa\rho\tau + k\kappa_{xt}}{\kappa k(k+\tau)}, \tag{19}$$
$$\gamma_2 = -\frac{\kappa_t}{k}, \tag{20}$$
$$\gamma_3 = \frac{\kappa\rho}{k^2} - \frac{\kappa\rho\tau + k\kappa_{xt}}{k^2(k+\tau)}. \tag{21}$$

The evolution of $\kappa$ and $\tau$ then satisfies

$$\kappa_t = \left[\frac{\kappa\rho}{k^2} - \frac{\kappa\rho\tau + k\kappa_{xt}}{k^2(k+\tau)}\right]_x - \frac{\tau\kappa_t}{k}, \tag{22}$$
$$\tau_t = \left[\frac{\kappa\rho\tau + k\kappa_{xt}}{\kappa k(k+\tau)}\right]_x + \frac{(\kappa^2)_t}{2k}. \tag{23}$$

Let us now introduce a new function $v$ by

$$v = k \int \frac{\gamma_3}{\kappa} dt. \tag{24}$$

It can be shown that the function $\kappa$ and $v$ satisfy the system

$$\kappa_{xt} = \kappa v_x v_t - 0.5\partial_x^{-1}[(|q|^2)_t]\kappa, \tag{25}$$

$$v_{xt} = -\frac{\kappa_t v_x}{\kappa_x v_t}. \tag{26}$$

Now, we define a new complex function

$$q = \kappa e^{iv}. \tag{27}$$

Then, $q$ satisfies the equation

$$q_{xt} + 0.5\partial_x^{-1}[(|q|^2)_t]q = 0. \tag{28}$$

This can also be written as

$$q_{xt} - \rho q = 0, \tag{29}$$

$$\rho_x + 0.5(|q|^2)_t = 0, \tag{30}$$

which is recognized as the focusing complex coupled dispersionless (CCD) system. Moreover, it is possible to derive the following constraint:

$$\rho^2 + \sigma|q_t|^2 = const \tag{31}$$

and, for simplicity,

$$\rho^2 + \sigma|q_t|^2 = 1, \tag{32}$$

meaning that

$$\rho = \pm\sqrt{1 - \sigma|q_t|^2}. \tag{33}$$

Therefore, the CCD system reduces to a single equation:

$$q_{xt} \mp \sqrt{1 - \sigma|q_t|^2}q = 0. \tag{34}$$

Although this system seems to involve two dependent variables $q$ and $\rho$, Equation (34) shows that it effectively contains only one, namely, $q(x, t)$.

## 4. Gauge Equivalent Counterpart

In Section 3, we established the geometrical (Lakshmanan-type) equivalence between the M-XIII equation in (2) and the CCD system in (29) and (30). In this section, we demonstrate that these equations are also gauge equivalent to each other.

Consider the gauge transformation

$$\Phi = g^{-1}\Psi, \quad \text{where} \quad g = \Psi|_{\lambda=k}.$$

Under this transformation, the function $\Psi$ satisfies the following Lax pair:

$$\Psi_x = U_2\Psi, \tag{35}$$
$$\Psi_t = V_2\Phi, \tag{36}$$

where the matrices $U_2$ and $V_2$ are provided by

$$U_2 = -i\lambda\sigma_3 + 0.5\begin{pmatrix} 0 & -q \\ \bar{q} & 0 \end{pmatrix}, \quad V_2 = \frac{i}{4\lambda}\left[\rho\sigma_3 + \begin{pmatrix} 0 & q_s \\ \bar{q}_s & 0 \end{pmatrix}\right].$$

The compatibility condition of this Lax pair is

$$\Psi_{xt} = \Psi_{tx},$$

which is equivalent to the following CCD system:

$$q_{xt} - \rho q = 0, \quad \rho_x + \frac{1}{2}(|q|^2)_t = 0.$$

Therefore, we can conclude that the M-XIII Equation (2) and the CCD system (29) and (30) are not only geometrically equivalent but also gauge equivalent.

This duality offers additional insight into the integrability of the M-XIII model and reveals its close structural relationship to other known dispersionless soliton equations.

## 5. Integrable Surfaces Related to the M-XIII Equation

In this section, we explore the connection between the M-XIII equation and the differential geometry of the surfaces. We show how the M-XIII equation induces integrable surface deformations through two distinct identifications.

### *5.1. Case 1:* $\mathbf{A} \equiv \mathbf{r}_x$

Let us first consider the identification

$$\mathbf{A} \equiv \mathbf{r}_x, \tag{37}$$

where $\mathbf{r}(x,t)$ is the position vector of the curve embedded on the surface. The identification $\mathbf{A} \equiv \mathbf{r}_x$ is commonly encountered in classical spin chain models such as the Heisenberg ferromagnet, where the spin vector is aligned with the tangent of a space curve. This interpretation also appears in elastic rod theory and nonlinear sigma models with geometrically constrained spin fields. Under this identification, the M-XIII equation in (2) takes the following form:

$$\mathbf{r}_t = \frac{1}{k}\mathbf{r}_x \wedge \mathbf{r}_{xt} + \frac{1}{k^2}\rho\mathbf{r}_x, \tag{38}$$
$$\rho_x = k\mathbf{A}\cdot(\mathbf{A}_t \wedge \mathbf{A}_x). \tag{39}$$

Equation (38) can also be written as

$$\mathbf{r}_{xt} + k\mathbf{r}_x \times \mathbf{r}_t = 0. \tag{40}$$

This equation describes the motion of a surface through the evolution of its position vector $\mathbf{r}(x,t)$. For the case with $k = -1$, this system reduces to a previously studied integrable model.

The corresponding Lax pair is provided by

$$\begin{aligned} F_x &= 0.5i(k-\lambda)r_xF = U_3F, \\ F_t &= \left[\frac{i(k-\lambda)}{2k\lambda}\rho r_x + \frac{(k-\lambda)}{2\lambda}r_xr_{xt}\right]F = V_3F. \end{aligned} \tag{41}$$

The compatibility condition leads to

$$\begin{aligned} ir_{xt} &= \frac{1}{4k}[r_x, r_{xt}]_x + \frac{i}{4k^2}\rho r_{xx}, \\ \rho_x &= -iktr(r_x \cdot [r_{xx}, r_{xt}]). \end{aligned}$$

From the geometric viewpoint, the function $\rho$ is related to the angle $\theta$ between the vector, that is, $\mathbf{r}_x$ and $\mathbf{r}_t$:

$$\rho = k\mathbf{r}_x \cdot \mathbf{r}_t = k\cos\theta. \tag{42}$$

Assuming $k = 1$ and $\sigma = 1$, Equations (32) and (42) yield

$$\rho = cos\theta, \quad q_t = \sin\theta e^{-\mathrm{i}\omega}, \tag{43}$$

where $\theta$ and $\omega$ are real-valued functions, leading to

$$q = (\theta_x - \mathrm{i}\omega_x \tan\theta)e^{-\mathrm{i}\omega}. \tag{44}$$

In terms of $\theta$ and $\omega$, the Lax pair in (35) and (36) becomes

$$U_2 = -i\lambda\sigma_3 + \begin{pmatrix} 0 & -\frac{1}{2}(\theta_x - \mathrm{i}\omega_x \tan\theta)e^{-\mathrm{i}\omega} \\ \frac{1}{2}(\theta_x + \mathrm{i}\omega_x \tan\theta)e^{\mathrm{i}\omega} & 0 \end{pmatrix}, \tag{45}$$

$$V_2 = \frac{\mathrm{i}}{4\lambda}\begin{pmatrix} \cos\theta & \sin\theta e^{-\mathrm{i}\omega} \\ \sin\theta e^{\mathrm{i}\omega} & -\cos\theta \end{pmatrix}. \tag{46}$$

Let us now return to the surface. Its fundamental forms read as follows [30]:

$$I = dx^2 + 2\cos\theta dxdt + dt^2, \tag{47}$$

$$II = (\tan\theta)\omega_x dx^2 + 2\sin\theta dxdt + (\sin\theta)\omega_t dt^2. \tag{48}$$

Now, we are ready to write the Gauss–Weingarten equations of the surface, for which we have the following [32]:

$$\mathbf{r}_{xx} = (\cot\theta)\theta_x\mathbf{r}_x - (\csc\theta)\theta_x\mathbf{r}_t - (\tan\theta)\omega_x\mathbf{N}, \tag{49}$$

$$\mathbf{r}_{xt} = \sin\theta\mathbf{N}\,, \tag{50}$$

$$\mathbf{r}_{tt} = -(\csc\theta)\theta_t\mathbf{r}_x + (\cot\theta)\theta_t\mathbf{r}_t + (\sin\theta)\omega_t\mathbf{N}, \tag{51}$$

$$\mathbf{N}_x = (\cot\theta + \csc\theta\sec\theta\omega_x)\mathbf{r}_x - (\csc\theta\omega_x + \csc\theta)\mathbf{r}_t, \tag{52}$$

$$\mathbf{N}_t = -(\csc\theta - \cot\theta\omega_t)\mathbf{r}_x + (\cot\theta + \csc\theta\omega_t)\mathbf{r}_t\,. \tag{53}$$

The compatibility conditions of these equations provide the following Mainardi–Codazzi equation:

$$(\omega_t\cos\theta)_x = \left(\frac{\omega_x}{\cos\theta}\right)_t. \tag{54}$$

At the same time, the Gaussian curvature of the surface reads as follows:

$$K = -\frac{(\tan\theta)\omega_x\omega_t + \sin\theta}{\sin\theta}. \tag{55}$$

The important formula follows from the Liouville–Beltrami form of the *Theorema egregium* and has the following form [30]:

$$\theta_{xt} - \sin\theta - (\tan\theta)\omega_x\omega_t = 0\,. \tag{56}$$

We can write the position vector on the surface in component form as

$$\mathbf{r} = (r_1, r_2, r_3) \tag{57}$$

or in matrix form as

$$r = r_1 e_1 + r_2 e_2 + r_3 e_3. \tag{58}$$

Now, following [45], we introduce three new matrices with the following forms:

$$T = \Phi^{-1} e_3 \Phi, \quad N = \Phi^{-1} e_2 \Phi, \quad B = \Phi^{-1} e_1 \Phi, \tag{59}$$

and with

$$e_j = \frac{1}{2\mathrm{i}}\sigma_j.$$

The above follows from the well-known formula

$$r_x = \Phi^{-1} U_\lambda \Phi\Big|_{\lambda=1}, \tag{60}$$

$$r_t = \Phi^{-1} V_\lambda \Phi\Big|_{\lambda=1}. \tag{61}$$

Thus, we finally have

$$r_x = \Phi^{-1} e_3 \Phi = T, \tag{62}$$

$$r_t = (\cos\theta)T + (\sin\theta\cos\omega)N + (\sin\theta\sin\omega)B, \tag{63}$$

where $x$ plays the role of the curve's arc length. These equations provide us with the following equation for the position vector $\mathbf{r}$ [30]:

$$\mathbf{r}_t = \rho\mathbf{r}_x + \mathbf{r}_x \wedge \mathbf{r}_{xt} \tag{64}$$

which after some transformation coincides with the $r$-form of the M-XIII equation in (40). Finally, we note that

$$\mathbf{r}_t^2 = \mathbf{r}_x^2 = 1, \tag{65}$$

or in matrix form,

$$r_t^2 = r_x^2 = I. \tag{66}$$

*5.2. Case 2:* $\mathbf{A} \equiv \mathbf{r}_t$

In this case, we consider an alternative identification

$$\mathbf{A} \equiv \mathbf{r}_t, \tag{67}$$

where $\mathbf{r}(x,t)$ is the position vector of the curve embedded on the surface and $t$ is the arclength parameter of the curve. The case with $\mathbf{A} \equiv \mathbf{r}_t$ corresponds to the surface evolution dynamics, where the spin vector evolves in time and is identified with the vector tangent to the time-like deformation of the surface. This is physically relevant in magnetoelastic

systems, filament dynamics, and models with curvature-induced spin transport. Then, the M-XIII equations in (8) and (9) take the form

$$\mathbf{r}_{tt} = k^{-1}\mathbf{r}_t \wedge \mathbf{r}_{xtt} + k^{-2}\rho \mathbf{r}_{xt}, \tag{68}$$

$$\rho_x = k\mathbf{r}_t \cdot (\mathbf{r}_{tt} \wedge \mathbf{r}_{xt}). \tag{69}$$

This equation defines some integrable surface in $R^3$. Note that Equations (68) and (69) are integrable with the following LR:

$$F_x = 0.5i(k-\lambda)r_t F = U_4 F, \tag{70}$$

$$F_t = \left[\frac{i(k-\lambda)}{2k\lambda}\rho r_t + \frac{(k-\lambda)}{2\lambda} r_t r_{tt}\right] F = V_4 F. \tag{71}$$

The compatibility condition of Equations (68) and (69) provides

$$ir_{tt} = 0.5k^{-1}[r_t, r_{tt}]_x + ik^{-2}\rho r_{xt}, \tag{72}$$

$$\rho_x = -0.5iktr(r_t \cdot [r_{xt}, r_{tt}]), \tag{73}$$

which is just the matrix form of Equations (68) and (69).

## 6. Soliton Solutions of the M-XIII Equation

We now present the simple one-soliton solution of the M-XIII equation in (2). This solution is constructed by utilizing the corresponding solution of the complex dispersionless (CCD) equation (see Equations (29) and (30)).

Let us consider the trivial seed solution for the CCD system:

$$q = 0, \quad \rho = 1. \tag{74}$$

Then, we have

$$U_2 = -i\lambda x\sigma_3, \quad V_2 = \frac{i}{4\lambda} t\sigma_3. \tag{75}$$

We can then apply the Sym–Tafel formula [31] to construct the corresponding surface:

$$r = \Phi^{-1}\Phi_\lambda\Big|_{\lambda=1}. \tag{76}$$

Using this approach, the explicit one-soliton surface is provided by

$$r_1 = \frac{b}{(1-a)^2+b^2} sechR \cos W, \tag{77}$$

$$r_2 = \frac{b}{(1-a)^2+b^2} sechR \sin W, \tag{78}$$

$$r_3 = \frac{b}{(1-a)^2+b^2} \tanh R + x + t, \tag{79}$$

where the functions $R$ and $W$ are defined as follows:

$$R = bx + \frac{b}{a^2+b^2}t, \quad W = (1-a)x + \left(1 + \frac{a}{a^2+b^2}\right)t.$$

This surface solution can be used to construct the one-soliton solution of the M-XIII equation in (2). The spin vector **A** components are obtained from the derivatives of the surface:

$$A_1 = r_{1x}, \quad A_2 = r_{2x}, \quad A_3 = r_{3x}. \tag{80}$$

These components represent the evolution of the spin field associated with the soliton surface. An example of the time evolution of the components $A1$, $A_2$, and $A_3$ is shown below in Figure 1.

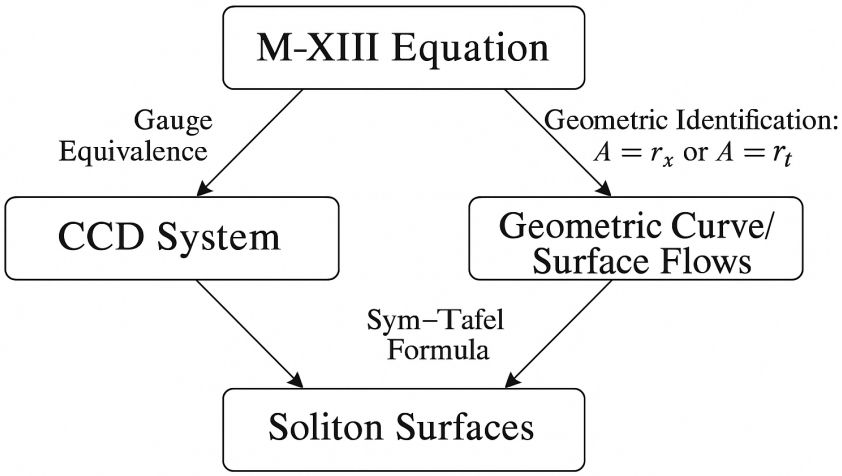


**Figure 1.** Commutative diagram illustrating the equivalence relations between the M-XIII equation, the CCD system, and the associated geometric and soliton surface models.

Figure 2 illustrates the 3D plots of the spin components $A_1$, $A_2$, and $A_3$ derived from the solution of a soliton surface. These components represent the spatial structure and evolution of the soliton in the M-XIII equation. The parameter values used here are $a = 0.5$ and $b = 1$, with $x \in [-10, 10]$ and $t \in [-5, 5]$. First, component $A_1$ shows localized oscillations along the $x$-axis, corresponding to the soliton envelope in the $r_1$-direction. Second, component $A_2$ captures the transverse rotational behavior of the soliton, which is characteristic of its internal spin structure. Third, component $A_3$ displays a kink-type profile representing the longitudinal polarization, and is often interpreted as the direction of magnetization in spin chain models.

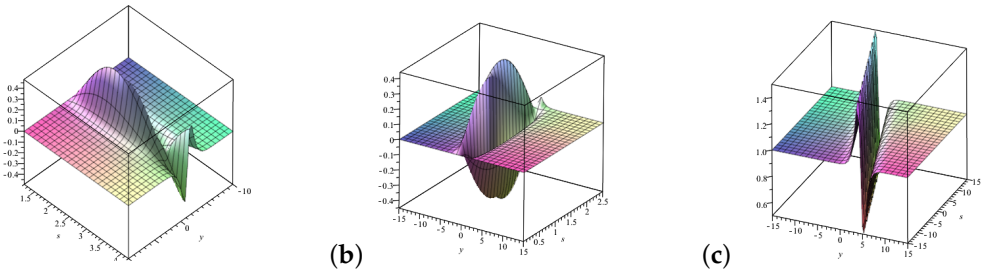


**Figure 2.** Component plots of the spin vector $\mathbf{A} = (A_1, A_2, A_3)$ derived from the one-soliton solution of the M-XIII equation for $a = 0.5$, $b = 1$, $x \in [-10, 10]$, and $t \in [-5, 5]$: (**a**) $A_1$, (**b**) $A_2$, (**c**) $A_3$.

## 7. Fractional CCD Equation

With

$$q_{xt} - pq = 0, \tag{81}$$

$$p_x + 0.5\left(|q|^2\right)_t = 0, \tag{82}$$

and using the definition and properties of the reduced M-partial derivative, Equation (81) can be rewritten as follows:

$$D_{M,xt}^{2\eta,\gamma} q - pq = 0, \tag{83}$$

$$D_{M,x}^{\eta,\gamma} p + 0,5 D_{M,t}^{\eta,\gamma} |q|^2 = 0, \tag{84}$$

where

$$D_{M,x}^{\eta,\gamma} f(x) = \lim_{\varepsilon \to 0} \frac{f\left(x E_\gamma(\varepsilon x^{1-\eta})\right) - f(x)}{\varepsilon}, \; 0 < \eta \leq 1, \; \gamma \in (0, \infty) \tag{85}$$

and where $E_\gamma(.)$ is the reduced Mittag–Leffler function.

The system in (84) involves nonlinear fractional-order partial differential equations, where $q = q(x,t)$ is a complex-valued wave function and $p = p(x,t)$ is a real-valued wave function. Using the reduced M-fractional derivative, we can derive the fractional form (84) of Equation (82). We construct a new class of soliton and soliton-type solutions along with their computational models using the Kudryashov method. The parameters $\eta$ and $\gamma$ in the M-fractional derivative play a crucial role in the behavior of the soliton solutions. The parameter $\eta$ governs the order of the nonlocal operator and affects the solution smoothness, while $\gamma$ modifies the scaling behavior in time. A detailed numerical investigation of the dependence of the soliton shape on these parameters will be considered in a future work.

### *7.1. Description of the Kudryashov Method*

Let us consider the following nonlinear partial differential equation:

$$S(h,\ h^2,\ h_x,\ h_t,\ h_{xx},\ h_{tt},\ h_{xt},\ \ldots) = 0. \tag{86}$$

Step 1: Applying the given wave transformations

$$h(x,t) = H(\omega), \qquad \omega = \delta x + \lambda t, \tag{87}$$

Equation (86) is reduced to the following ordinary differential equations:

$$T(H,\ H',\ H'',\ \ldots,) = 0. \tag{88}$$

Step 2: The solution of Equation (88) is sought in the form

$$H(\omega) = a_0 + \sum_{j=1}^{M} \frac{a_j}{(1+\phi(\omega))^j}, \tag{89}$$

where $a_j (j = 0,\ 1,\ 2,\ 3,\ \ldots,\ M)$ are coefficients to be determined. The value of the upper summation index $M$ is obtained using the homogeneous balance method. The new function $\phi(\omega)$ satisfies the following auxiliary differential equation:

$$\phi'(\omega) = \rho + \sigma\phi(\omega) + \Omega\phi^2(\omega), \tag{90}$$

where $\rho,\ \sigma$, and $\Omega$ are constants. The set of solutions to Equation (90) is classified according to the possible values of these constants [46].

If $\rho \neq 0$, $\sigma \neq 0$, and $\Omega \neq 0$, then the solution set takes the following form:

$$\phi(\omega) = \frac{1}{2\Omega}\left(\sqrt{4\rho\Omega - \sigma^2}\,\mathrm{tg}\left(\frac{1}{2}\sqrt{4\rho\Omega - \sigma^2}(d_0 + \omega)\right) - \sigma\right), \;\; 4\rho\Omega > \sigma^2, \tag{91}$$

$$\phi(\omega) = \frac{-1}{2\Omega}\left(\sqrt{4\rho\Omega - \sigma^2}\mathrm{ctg}\left(\frac{1}{2}\sqrt{4\rho\Omega - \sigma^2}(d_0+\omega)\right) + \sigma\right), \ 4\rho\Omega > \sigma^2, \tag{92}$$

$$\phi(\omega) = \frac{-1}{2\Omega}\left(\sqrt{4\rho\Omega - \sigma^2}\mathrm{th}\left(\frac{1}{2}\sqrt{4\rho\Omega - \sigma^2}(d_0+\omega)\right) + \sigma\right), \ 4\rho\Omega < \sigma^2, \tag{93}$$

$$\phi(\omega) = \frac{-1}{2\Omega}\left(\sqrt{4\rho\Omega - \sigma^2}\mathrm{cth}\left(\frac{1}{2}\sqrt{4\rho\Omega - \sigma^2}(d_0+\omega)\right) + \sigma\right), \ 4\rho\Omega < \sigma^2, \tag{94}$$

$$\phi(\omega) = \frac{-1}{\Omega}\left(\frac{1}{d_0+\omega} + \frac{\sigma}{2}\right), \ 4\rho\Omega = \sigma^2. \tag{95}$$

If $\rho = 0$ and $\Omega \neq 0$, then we have

$$\phi(\omega) = \frac{-1}{2\Omega}\left(\sigma\mathrm{th}\left(\frac{\sigma}{2}(d_0+\omega)\right) + \sigma\right), \sigma^2 > 0, \tag{96}$$

$$\phi(\omega) = \frac{-1}{2\Omega}\left(\sigma\mathrm{cth}\left(\frac{\sigma}{2}(d_0+\omega)\right) + \sigma\right), \sigma^2 > 0, \tag{97}$$

$$\phi(\omega) = \frac{1}{2\Omega}\left(\sqrt{-\sigma^2}\mathrm{tg}\left(\frac{\sqrt{-\sigma^2}}{2}(d_0+\omega)\right) - \sigma\right), \sigma^2 < 0, \tag{98}$$

$$\phi(\omega) = \frac{-1}{2\Omega}\left(\sqrt{-\sigma^2}\mathrm{ctg}\left(\frac{\sqrt{-\sigma^2}}{2}(d_0+\omega)\right) + \sigma\right), \sigma^2 < 0, \tag{99}$$

$$\phi(\omega) = \frac{\sigma}{\sigma e^{-\sigma(d_0+\omega)} - \Omega}, \ \sigma \neq 0, \tag{100}$$

$$\phi(\omega) = \frac{-1}{\Omega\omega}, \ \sigma = 0. \tag{101}$$

If $\sigma = 0$ and $\Omega \neq 0$, we have

$$\phi(\omega) = \frac{\sqrt{\rho\Omega}}{\Omega}\mathrm{tg}\left(\sqrt{\rho\Omega}(d_0+\omega)\right), \rho\Omega > 0, \tag{102}$$

$$\phi(\omega) = -\frac{\sqrt{\rho\Omega}}{\Omega}\mathrm{ctg}\left(\sqrt{\rho\Omega}(d_0+\omega)\right), \rho\Omega > 0, \tag{103}$$

$$\phi(\omega) = -\frac{\sqrt{\rho\Omega}}{\Omega}\mathrm{th}\left(\sqrt{-\rho\Omega}(d_0+\omega)\right), \rho\Omega < 0, \tag{104}$$

$$\phi(\omega) = -\frac{\sqrt{\rho\omega}}{\Omega}\mathrm{cth}\left(\sqrt{-\rho\Omega}(d_0+\omega)\right), \rho\Omega < 0, \tag{105}$$

$$\phi(\omega) = -\frac{1}{\Omega(d_0+\omega)}, \ \rho = 0. \tag{106}$$

Finally, if $\Omega = 0$ and $\sigma \neq 0$, we have

$$\phi(\omega) = \frac{1}{\sigma}\left(e^{\sigma(d_0+\omega)} - \rho\right). \tag{107}$$

Step 3: By substituting Equation (89) into Equation (88) and collecting all coefficients of powers of $\phi(\omega)$ that vanish, we obtain a system of algebraic equations involving unknowns $a_0, a_j, \ (j = 1, 2, \ldots m)$ and other parameters.

Step 4: Solving the resulting algebraic system, we obtain exact solutions of the fractional equation in (84).

*7.2. Solutions of the Fractional Nonlinear Schrödinger Equation*

In this subsection, we construct exact solutions of the fractional nonlinear Schrödinger equation with a compatible potential using the Kudryashov method. To this end, we consider the following transformations:

$$q(x,t) = F(\omega)\, e^{i\psi}, \tag{108}$$

$$p(x,t) = G(\omega), \tag{109}$$

where $F(\omega)$ represents the pulse shape

$$\psi = \frac{\Gamma(1+\gamma)}{\eta}(\lambda t^{\eta} - a x^{\eta}), \tag{110}$$

$$\omega = \frac{\Gamma(1+\gamma)}{\eta}(x^{\eta} - \tau t^{\eta}), \tag{111}$$

where $a$ is the soliton frequency, $\lambda$ is the soliton wavenumber, and $\tau$ represents the soliton velocity.

Taking into account the above notation, we can reduce the system of Equation (84) into an ordinary differential equation in terms of the new variable $\omega$.

Equation (84) is transformed into the form

$$\begin{aligned} D^{2\eta,\gamma}_{M,xt} q &= \frac{x^{1-\eta}}{\Gamma(\gamma+1)} \frac{d D^{\eta,\gamma}_{M,t} q}{dx} = \\ &= \frac{x^{1-\eta}}{\Gamma(\gamma+1)} \left[ e^{i\psi} \frac{d(i\lambda F - \tau F')}{dx} + (i\lambda F - \tau F') \frac{d(e^{i\psi})}{dx} \right] = \\ &= \frac{x^{1-\eta}}{\Gamma(\gamma+1)} e^{i\psi} \left[ \frac{d(i\lambda F - \tau F')}{d\omega} \frac{d\omega}{dx} + i(i\lambda F - \tau F') \frac{\Gamma(1+\gamma)}{\eta} \left( -a\eta x^{\eta-1} \right) \right] = \\ &= \frac{x^{1-\eta}}{\Gamma(\gamma+1)} e^{i\psi} \left[ \frac{\Gamma(1+\gamma)}{\eta} \eta x^{\eta-1} (i\lambda F' - \tau F'') - ia\eta x^{\eta-1} (i\lambda F - \tau F') \frac{\Gamma(1+\gamma)}{\eta} \right] = \\ &= e^{i\psi} \left[ i\lambda F' - \tau F'' + a\lambda F + ia\tau F' \right]. \end{aligned} \tag{112}$$

Thus,

$$D^{2\eta,\gamma}_{M,xt} q = (i\lambda F' - \tau F'' + a\lambda F + ia\tau F') e^{i\psi}. \tag{113}$$

Next, we proceed to the second equation of the system in (84):

$$D^{\eta,\gamma}_{M,x} p = D^{\eta,\gamma}_{M,t} G = \frac{x^{1-\eta}}{\Gamma(\gamma+1)} \frac{dG}{dx} = \frac{x^{1-\eta}}{\Gamma(\gamma+1)} \frac{dG}{d\omega} \frac{d\omega}{dx} = \frac{x^{1-\eta}}{\Gamma(\gamma+1)} \frac{\Gamma(\gamma+1)}{\eta} \eta x^{\eta-1} G' = G'. \tag{114}$$

Therefore,

$$D^{\eta,\gamma}_{M,x} p = G' \tag{115}$$

and

$$\begin{aligned} D^{\eta,\gamma}_{M,t} \left( |q|^2 \right) &= D^{\eta,\gamma}_{M,t} \left[ F e^{i\psi} \cdot F e^{-i\psi} \right] = \\ &= D^{\eta,\gamma}_{M,t} F^2 = \frac{t^{1-\eta}}{\Gamma(\gamma+1)} \frac{dF^2}{dt} = \frac{t^{1-\eta}}{\Gamma(\gamma+1)} \frac{\Gamma(\gamma+1)}{\eta} \left( -\tau\eta t^{\eta-1} \right) \cdot 2FF' = -2\tau FF'. \end{aligned} \tag{116}$$

Hence, we obtain

$$D^{\eta,\gamma}_{M,t} \left( |q|^2 \right) = -2\tau FF'. \tag{117}$$

By applying the transformation to the new variable (111), the system of nonlinear fractional partial differential equations in (84) is reduced to the following system of ordinary differential equations:

$$a\lambda F + i(\lambda + a\tau)F^{'} - \tau F'' - FG = 0, \tag{118}$$

$$G^{'} - \tau F F^{'} = 0. \tag{119}$$

Next, by integrating the second equation in (119) with respect to $\omega$ and omitting the integration constant we obtain

$$G(\omega) = \frac{1}{2}\tau F^2(\omega). \tag{120}$$

Substituting (120) into the first equation of the system in (119), we separate the real and imaginary parts.
Real part:

$$a\lambda F - \tau F'' - \frac{1}{2}\tau F^3 = 0. \tag{121}$$

Imaginary part:

$$(\lambda + a\tau)F^{'} = 0. \tag{122}$$

From Equation (122), we obtain

$$\lambda = -a\tau. \tag{123}$$

Substituting Equations (120) and (123) into (121) yields

$$a^2 F + F'' + \frac{1}{2}F^3 = 0. \tag{124}$$

We now apply the homogeneous balance method to Equation (124) in order to determine the highest order $M$ in the summation form of the solution (89). For this, we assume a solution of the form $F = \omega^{-M}$ and take the second derivative; hence, the solution in the form of (89) becomes

$$F = \alpha_0 + \frac{\alpha_1}{1 + \phi}, \tag{125}$$

where $\alpha_0$ and $\alpha_1$ are undetermined constants. By substituting Equations (90) and (125) into Equation (124), we obtain the following set of solutions:

$$\alpha_0 = \pm\sqrt{2}ia, \tag{126}$$

$$\alpha_1 = \pm\frac{2}{i}\left(\rho + \sigma\phi + \Omega\phi^2\right). \tag{127}$$

Next, by successively substituting the solutions for $\phi$ from Equations (91)–(107) into (125), we obtain the following families of solution pairs.

Case 1: If $\rho \neq 0$, $\sigma \neq 0$, and $\Omega \neq 0$, we have

$$q(x,t) = \pm e^{i\psi} \cdot \left( \sqrt{2}ia + \frac{2\left(\rho + \frac{\sigma}{2\Omega}\left(N\mathrm{tg}\left(\frac{1}{2}Nz\right) - \sigma\right) + \frac{1}{4\Omega}\left(N\mathrm{tg}\left(\frac{1}{2}Nz\right) - \sigma\right)^2\right)}{i\left(1 + \frac{1}{2\Omega}\left(N\mathrm{tg}\left(\frac{1}{2}Nz\right) - \sigma\right)\right)} \right), \tag{128}$$

$$p(x,t) = -a^2 + \frac{2\sqrt{2}a\left(\rho + \frac{\sigma\left(N\mathrm{tg}\left(\frac{1}{2}Nz\right) - \sigma\right)}{2\Omega} + \frac{\left(N\mathrm{tg}\left(\frac{1}{2}Nz\right) - \sigma\right)^2}{4\Omega}\right)}{1 + \frac{1}{2\Omega}\left(N\mathrm{tg}\left(\frac{1}{2}Nz\right) - \sigma\right)} - \tag{129}$$
$$- \frac{2\left(\rho + \frac{\sigma}{2\Omega}\left(N\mathrm{tg}\left(\frac{1}{2}Nz\right) - \sigma\right) + \frac{1}{4\Omega}\left(N\mathrm{tg}\left(\frac{1}{2}Nz\right) - \sigma\right)^2\right)^2}{\left(1 + \frac{1}{2\Omega}\left(N\mathrm{tg}\left(\frac{1}{2}Nz\right) - \sigma\right)\right)^2},$$

$$q(x,t) = \pm e^{i\psi} \cdot \left(\sqrt{2}ia + \frac{2\left(\rho - \frac{\sigma}{2\Omega}\left(N\mathrm{ctg}\left(\frac{1}{2}Nz\right) + \sigma\right) + \frac{\left(N\mathrm{ctg}\left(\frac{1}{2}Nz\right) + \sigma\right)^2}{4\Omega}\right)}{i\left(1 - \frac{1}{2\Omega}\left(N\mathrm{ctg}\left(\frac{1}{2}Nz\right) + \sigma\right)\right)}\right), \tag{130}$$

$$p(x,t) = -a^2 + \frac{2\sqrt{2}a\left(\rho - \frac{\sigma}{2\Omega}\left(N\mathrm{ctg}\left(\frac{1}{2}Nz\right) + \sigma\right) + \frac{\left(N\mathrm{ctg}\left(\frac{1}{2}Nz\right) + \sigma\right)^2}{4\Omega}\right)}{1 - \frac{1}{2\Omega}\left(N\mathrm{ctg}\left(\frac{1}{2}Nz\right) + \sigma\right)} - \tag{131}$$
$$- \frac{2\left(\rho - \frac{\sigma}{2\Omega}\left(N\mathrm{ctg}\left(\frac{1}{2}Nz\right) + \sigma\right) + \frac{\left(N\mathrm{ctg}\left(\frac{1}{2}Nz\right) + \sigma\right)^2}{4\Omega}\right)^2}{\left(1 - \frac{1}{2\Omega}\left(N\mathrm{ctg}\left(\frac{1}{2}Nz\right) + \sigma\right)\right)^2},$$

$$q(x,t) = \pm e^{i\psi} \cdot \left(\sqrt{2}ia + \frac{2\left(\rho - \frac{\sigma}{2\Omega}\left(N\mathrm{th}\left(\frac{1}{2}Nz\right) + \sigma\right) + \frac{1}{4\Omega}\left(\left(N\mathrm{th}\left(\frac{1}{2}Nz\right) + \sigma\right)\right)^2\right)}{i\left(1 - \frac{1}{2\Omega}\left(N\mathrm{th}\left(\frac{1}{2}Nz\right) + \sigma\right)\right)}\right), \tag{132}$$

$$p(x,t) = -a^2 + \frac{2\sqrt{2}a\left(\rho - \frac{\sigma}{2\Omega}\left(N\mathrm{th}\left(\frac{1}{2}Nz\right) + \sigma\right) + \frac{\left(N\mathrm{th}\left(\frac{1}{2}Nz\right) + \sigma\right)^2}{4\Omega}\right)}{1 - \frac{1}{2\Omega}\left(N\mathrm{th}\left(\frac{1}{2}Nz\right) + \sigma\right)} - \tag{133}$$
$$- \frac{2\left(\rho - \frac{\sigma}{2\Omega}\left(N\mathrm{th}\left(\frac{1}{2}Nz\right) + \sigma\right) + \frac{\left(N\mathrm{th}\left(\frac{1}{2}Nz\right) + \sigma\right)^2}{4\Omega}\right)^2}{\left(1 - \frac{1}{2\Omega}\left(N\mathrm{th}\left(\frac{1}{2}Nz\right) + \sigma\right)\right)^2},$$

$$q(x,t) = \pm e^{i\psi} \cdot \left(\sqrt{2}ia + \frac{2\left(\rho - \frac{\sigma}{2\Omega}\left(N\mathrm{cth}\left(\frac{1}{2}Nz\right) + \sigma\right) + \frac{1}{4\Omega}\left(\left(N\mathrm{cth}\left(\frac{1}{2}Nz\right) + \sigma\right)\right)^2\right)}{i\left(1 - \frac{1}{2\Omega}\left(N\mathrm{cth}\left(\frac{1}{2}Nz\right) + \sigma\right)\right)}\right), \tag{134}$$

$$p(x,t) = -a^2 + \frac{2\sqrt{2}a\left(\rho - \frac{\sigma}{2\Omega}\left(N\mathrm{cth}\left(\frac{1}{2}Nz\right) + \sigma\right) + \frac{\left(N\mathrm{cth}\left(\frac{1}{2}Nz\right) + \sigma\right)^2}{4\Omega}\right)}{1 - \frac{1}{2\Omega}\left(N\mathrm{cth}\left(\frac{1}{2}Nz\right) + \sigma\right)} - \tag{135}$$
$$- \frac{2\left(\rho - \frac{\sigma}{2\Omega}\left(N\mathrm{cth}\left(\frac{1}{2}Nz\right) + \sigma\right) + \frac{\left(N\mathrm{cth}\left(\frac{1}{2}Nz\right) + \sigma\right)^2}{4\Omega}\right)^2}{\left(1 - \frac{1}{2\Omega}\left(N\mathrm{cth}\left(\frac{1}{2}Nz\right) + \sigma\right)\right)^2},$$

where

$$N = \sqrt{4\rho\Omega - \sigma^2}.$$

Case 2: If $\rho = 0$ and $\Omega \neq 0$, we have

$$q(x,t) = \pm e^{i\psi}\left(\sqrt{2}ia + \frac{2\left(\rho - \frac{\sigma^2}{2\Omega}\left(\mathrm{th}\left(\frac{\sigma}{2}z\right) + 1\right) + \frac{\sigma}{4\Omega}\left(\mathrm{th}\left(\frac{\sigma}{2}z\right) + 1\right)^2\right)}{i\left(1 - \frac{\sigma}{2\Omega}\left(\mathrm{th}\left(\frac{\sigma}{2}z\right) + 1\right)\right)}\right), \tag{136}$$

$$p(x,t) = -a^2 + \frac{2\sqrt{2}a\left(\rho - \frac{\sigma^2}{2\Omega}\left(\mathrm{th}\left(\frac{\sigma}{2}z\right) + 1\right) + \frac{\left(\sigma \mathrm{th}\left(\frac{\sigma}{2}z\right) + \sigma\right)^2}{4\Omega}\right)}{1 - \frac{\sigma}{2\Omega}\left(\mathrm{th}\left(\frac{\sigma}{2}z\right) + 1\right)} - \tag{137}$$

$$- \frac{2\left(\rho - \frac{\sigma^2}{2\Omega}\left(\mathrm{th}\left(\frac{\sigma}{2}z\right) + 1\right) + \frac{\left(\left(\sigma \mathrm{th}\left(\frac{\sigma}{2}z\right) + \sigma\right)\right)^2}{4\Omega}\right)^2}{\left(1 - \frac{\sigma}{2\Omega}\left(\mathrm{th}\left(\frac{\sigma}{2}z\right) + 1\right)\right)^2},$$

$$q(x,t) = \pm e^{i\psi}\left(\sqrt{2}ia + \frac{2\left(\rho - \frac{\sigma^2}{2\Omega}\left(\mathrm{cth}\left(\frac{\sigma}{2}z\right) + 1\right) + \frac{\sigma}{4\Omega}\left(\mathrm{cth}\left(\frac{\sigma}{2}z\right) + 1\right)^2\right)}{i\left(1 - \frac{\sigma}{2\Omega}\left(\mathrm{cth}\left(\frac{\sigma}{2}z\right) + 1\right)\right)}\right), \tag{138}$$

$$p(x,t) = -a^2 + \frac{2\sqrt{2}a\left(\rho - \frac{\sigma^2}{2\Omega}\left(\mathrm{cth}\left(\frac{\sigma}{2}z\right) + 1\right) + \frac{\left(\sigma \mathrm{cth}\left(\frac{\sigma}{2}z\right) + \sigma\right)^2}{4\Omega}\right)}{1 - \frac{\sigma}{4\Omega}\left(\mathrm{cth}\left(\frac{\sigma}{2}z\right) + 1\right)} - \tag{139}$$

$$- \frac{2\left(\rho - \frac{\sigma^2}{2\Omega}\left(\mathrm{cth}\left(\frac{\sigma}{2}z\right) + 1\right) + \frac{\left(\left(\sigma \mathrm{cth}\left(\frac{\sigma}{2}z\right) + \sigma\right)\right)^2}{4\Omega}\right)^2}{\left(1 - \frac{\sigma}{2\Omega}\left(\mathrm{cth}\left(\frac{\sigma}{2}z\right) + 1\right)\right)^2},$$

$$q(x,t) = \pm e^{i\psi}\left(\sqrt{2}ia + \frac{2\left(\rho + \frac{\sigma}{2\Omega}\left(\sqrt{-\sigma^2}\mathrm{tg}\left(\frac{\sqrt{-\sigma^2}}{2}z\right) - \sigma\right) + \frac{1}{4\Omega}\left(\sqrt{-\sigma^2}\mathrm{tg}\left(\frac{\sqrt{-\sigma^2}}{2}z\right) - \sigma\right)^2\right)}{i\left(1 + \frac{1}{2\Omega}\left(\sqrt{-\sigma^2}\mathrm{tg}\left(\frac{\sqrt{-\sigma^2}}{2}z\right) - \sigma\right)\right)}\right), \tag{140}$$

$$p(x,t) = -a^2 + \frac{2\sqrt{2}a\left(\rho + \frac{\sigma}{2\Omega}\left(\sqrt{-\sigma^2}\mathrm{tg}\left(\frac{\sqrt{-\sigma^2}}{2}z\right) - \sigma\right) + \frac{1}{4\Omega}\left(\sqrt{-\sigma^2}\mathrm{tg}\left(\frac{\sqrt{-\sigma^2}}{2}z\right) - \sigma\right)^2\right)}{1 + \frac{1}{2\Omega}\left(\sqrt{-\sigma^2}\mathrm{tg}\left(\frac{\sqrt{-\sigma^2}}{2}z\right) - \sigma\right)} - \tag{141}$$

$$- \frac{2\left(\rho + \frac{\sigma}{2\Omega}\left(\sqrt{-\sigma^2}\mathrm{tg}\left(\frac{\sqrt{-\sigma^2}}{2}z\right) - \sigma\right) + \frac{1}{4\Omega}\left(\sqrt{-\sigma^2}\mathrm{tg}\left(\frac{\sqrt{-\sigma^2}}{2}z\right) - \sigma\right)^2\right)^2}{\left(1 + \frac{1}{2\Omega}\left(\sqrt{-\sigma^2}\mathrm{tg}\left(\frac{\sqrt{-\sigma^2}}{2}z\right) - \sigma\right)\right)^2},$$

$$q(x,t) = \pm e^{i\psi}\left(\sqrt{2}\mathrm{ia} + \frac{2\left(\rho - \frac{\sigma}{2\Omega}\left(\sqrt{-\sigma^2}\mathrm{ctg}\left(\frac{\sqrt{-\sigma^2}}{2}z\right) + \sigma\right) + \frac{1}{4\Omega}\left(\sqrt{-\sigma^2}\mathrm{ctg}\left(\frac{\sqrt{-\sigma^2}}{2}z\right) + \sigma\right)^2\right)}{i\left(1 - \frac{1}{2\Omega}\left(\sqrt{-\sigma^2}\mathrm{ctg}\left(\frac{\sqrt{-\sigma^2}}{2}z\right) + \sigma\right)\right)}\right), \tag{142}$$

$$p(x,t) = -a^2 + \frac{2\sqrt{2}a\left(\rho - \frac{\sigma}{2\Omega}\left(\sqrt{-\sigma^2}\mathrm{ctg}\left(\frac{\sqrt{-\sigma^2}}{2}z\right) + \sigma\right) + \frac{1}{4\Omega}\left(\sqrt{-\sigma^2}\mathrm{ctg}\left(\frac{\sqrt{-\sigma^2}}{2}z\right) + \sigma\right)^2\right)}{\left(1 - \frac{1}{2\Omega}\left(\sqrt{-\sigma^2}\mathrm{ctg}\left(\frac{\sqrt{-\sigma^2}}{2}z\right) + \sigma\right)\right)} - \tag{143}$$

$$- \frac{2\left(\rho - \frac{\sigma}{2\Omega}\left(\sqrt{-\sigma^2}\mathrm{ctg}\left(\frac{\sqrt{-\sigma^2}}{2}z\right) + \sigma\right) + \frac{1}{4\Omega}\left(\sqrt{-\sigma^2}\mathrm{ctg}\left(\frac{\sqrt{-\sigma^2}}{2}z\right) + \sigma\right)^2\right)^2}{\left(1 - \frac{1}{2\Omega}\left(\sqrt{-\sigma^2}\mathrm{ctg}\left(\frac{\sqrt{-\sigma^2}}{2}z\right) + \sigma\right)\right)^2},$$

$$q(x,t) = \pm e^{i\psi}\left(\sqrt{2}ia + \frac{2\left(\rho + \frac{\sigma^2}{\sigma \mathrm{e}^{-\sigma z} - \Omega} + \Omega\left(\frac{\sigma}{\sigma \mathrm{e}^{-\sigma z} - \Omega}\right)^2\right)}{i\left(1 + \frac{\sigma}{\sigma \mathrm{e}^{-\sigma z} - \Omega}\right)}\right), \tag{144}$$

$$p(x,t) = -a^2 + \frac{2\sqrt{2}a\left(\rho + \frac{\sigma^2}{\sigma \mathrm{e}^{-\sigma z}\Omega} + \Omega\left(\frac{\sigma}{\sigma \mathrm{e}^{-\sigma z} - \Omega}\right)^2\right)}{1 + \frac{\sigma}{\sigma \mathrm{e}^{-\sigma z} - \Omega}} - \frac{2\left(\rho + \frac{\sigma^2}{\sigma \mathrm{e}^{-\sigma z} - \Omega} + \Omega\left(\frac{\sigma}{\sigma \mathrm{e}^{-\sigma z} - \Omega}\right)^2\right)^2}{\left(1 + \frac{\sigma}{\sigma \mathrm{e}^{-\sigma z} - \Omega}\right)^2}, \tag{145}$$

$$q(x,t) = \pm e^{i\psi}\left(\sqrt{2}ia + \frac{2\left(\rho - \frac{\sigma}{\Omega\omega} + \frac{1}{\Omega\omega^2}\right)}{i\left(1 - \frac{1}{\Omega\omega}\right)}\right), \tag{146}$$

$$p(x,t) = -a^2 + \frac{2\sqrt{2}a\left(\rho - \frac{\sigma}{\Omega\omega} + \frac{1}{\Omega\omega^2}\right)}{1 - \frac{1}{\Omega\omega}} - \frac{2\left(\rho - \frac{\sigma}{\Omega\omega} + \frac{1}{\Omega\omega^2}\right)^2}{\left(1 - \frac{1}{\Omega\omega}\right)^2}, \tag{147}$$

where

$$\psi = \frac{\Gamma(1+\gamma)}{\eta}\left(-ax^\eta + \left(\frac{2a\theta_1 + \tau - a\theta_2\tau}{\theta_2}\right)t^\eta\right).$$

Case 3: If $\sigma = 0$ and $\Omega \neq 0$, we have

$$q(x,t) = \pm e^{i\psi}\left(\sqrt{2}ia + \frac{2\left(\rho + \sigma\frac{\sqrt{\rho\Omega}}{\Omega}\mathrm{tg}(\sqrt{\rho\Omega}z) \ + \rho\ \mathrm{tg}^2(\sqrt{\rho\Omega}z)\right)}{i\left(1 + \frac{\sqrt{\rho\Omega}}{\Omega}\mathrm{tg}(\sqrt{\rho\Omega}z)\right)}\right), \tag{148}$$

$$p(x,t) = -a^2 + \frac{2\sqrt{2}a\left(\rho + \sigma\frac{\sqrt{\rho\Omega}}{\Omega}\mathrm{tg}(\sqrt{\rho\Omega}z) \ + \rho\ \mathrm{tg}^2(\sqrt{\rho\Omega}z)\right)}{1 + \frac{\sqrt{\rho\Omega}}{\Omega}\mathrm{tg}(\sqrt{\rho\Omega}z)} - \frac{2\left(\rho + \sigma\frac{\sqrt{\rho\Omega}}{\Omega}\mathrm{tg}(\sqrt{\rho\Omega}z) \ + \rho\ \mathrm{tg}^2(\sqrt{\rho\Omega}z)\right)^2}{\left(1 + \frac{\sqrt{\rho\Omega}}{\Omega}\mathrm{tg}(\sqrt{\rho\Omega}z)\right)^2}, \tag{149}$$

$$q(x,t) = \pm e^{i\psi}\left(\sqrt{2}ia + \frac{2\left(\rho - \sigma\frac{\sqrt{\rho\Omega}}{\Omega}\mathrm{ctg}(\sqrt{\rho\Omega}z) \ + \rho\ c\mathrm{tg}^2(\sqrt{\rho\Omega}z)\right)}{i\left(1 - \frac{\sqrt{\rho\Omega}}{\Omega}\mathrm{ctg}(\sqrt{\rho\Omega}z)\right)}\right), \tag{150}$$

$$p(x,t) = -a^2 + \frac{2\sqrt{2}a\left(\rho - \sigma\frac{\sqrt{\rho\Omega}}{\Omega}\mathrm{ctg}(\sqrt{\rho\Omega}z) \ + \rho\ c\mathrm{tg}^2(\sqrt{\rho\Omega}z)\right)}{1 - \frac{\sqrt{\rho\Omega}}{\Omega}\mathrm{ctg}(\sqrt{\rho\Omega}z)} - \frac{2\left(\rho - \sigma\frac{\sqrt{\rho\Omega}}{\Omega}\mathrm{ctg}(\sqrt{\rho\Omega}z) \ + \rho\ c\mathrm{tg}^2(\sqrt{\rho\Omega}z)\right)^2}{\left(1 - \frac{\sqrt{\rho\Omega}}{\Omega}\mathrm{ctg}(\sqrt{\rho\Omega}z)\right)^2}, \tag{151}$$

$$q(x,t) = \pm e^{i\psi}\left(\sqrt{2}ia + \frac{2\left(\rho - \sigma\frac{\sqrt{\rho\Omega}}{\Omega}\mathrm{th}(\sqrt{-\rho\Omega}z) \ + \rho\ \mathrm{th}^2(\sqrt{-\rho\Omega}z)\right)}{i\left(1 - \frac{\sqrt{\rho\Omega}}{\Omega}\mathrm{th}(\sqrt{-\rho\Omega}z)\right)}\right), \tag{152}$$

$$p(x,t) = -a^2 + \frac{2\sqrt{2}a\left(\rho - \sigma\frac{\sqrt{\rho\Omega}}{\Omega}\mathrm{th}(\sqrt{-\rho\Omega}z) \ + \rho\ \mathrm{th}^2(\sqrt{-\rho\Omega}z)\right)}{1 - \frac{\sqrt{\rho\Omega}}{\Omega}\mathrm{th}(\sqrt{-\rho\Omega}z)} - \frac{2\left(\rho - \sigma\frac{\sqrt{\rho\Omega}}{\Omega}\mathrm{th}(\sqrt{-\rho\Omega}z) \ + \rho\ \mathrm{th}^2(\sqrt{-\rho\Omega}z)\right)^2}{\left(1 - \frac{\sqrt{\rho\Omega}}{\Omega}\mathrm{th}(\sqrt{-\rho\Omega}z)\right)^2}, \tag{153}$$

$$q(x,t) = \pm e^{i\psi}\left(\sqrt{2}\mathrm{ia}+\frac{2\left(\rho-\sigma\frac{\sqrt{\rho\Omega}}{\Omega}\mathrm{cth}\left(\sqrt{-\rho\Omega}z\right)\ +\rho\ \mathrm{cth}^2\left(\sqrt{-\rho\Omega}z\right)\right)}{i\left(1-\frac{\sqrt{\rho\Omega}}{\Omega}\mathrm{cth}\left(\sqrt{-\rho\Omega}z\right)\right)}\right), \tag{154}$$

$$p(x,t) = -a^2+\frac{2\sqrt{2}a\left(\rho-\sigma\frac{\sqrt{\rho\Omega}}{\Omega}\mathrm{cth}\left(\sqrt{-\rho\Omega}z\right)\ +\rho\ \mathrm{cth}^2\left(\sqrt{-\rho\Omega}z\right)\right)}{1-\frac{\sqrt{\rho\Omega}}{\Omega}\mathrm{cth}\left(\sqrt{-\rho\Omega}z\right)}- \tag{155}$$
$$-\frac{2\left(\rho-\sigma\frac{\sqrt{\rho\Omega}}{\Omega}\mathrm{cth}\left(\sqrt{-\rho\Omega}z\right)\ +\rho\ \mathrm{cth}^2\left(\sqrt{-\rho\Omega}z\right)\right)^2}{\left(1-\frac{\sqrt{\rho\Omega}}{\Omega}\mathrm{cth}\left(\sqrt{-\rho\Omega}z\right)\right)^2},$$

$$q(x,t) = \pm e^{i\psi}\left(\sqrt{2}\mathrm{ia}+\frac{2\left(\rho-\frac{\sigma}{\Omega z}+\frac{1}{\Omega z^2}\right)}{i\left(1-\frac{1}{\Omega z}\right)}\right), \tag{156}$$

$$p(x,t) = -a^2+\frac{2\sqrt{2}a\left(\rho-\frac{\sigma}{\Omega z}+\frac{1}{\Omega z^2}\right)}{1-\frac{1}{\Omega z}}-\frac{2\left(\rho-\frac{\sigma}{\Omega z}+\frac{1}{\Omega z^2}\right)^2}{\left(1-\frac{1}{\Omega z}\right)^2}. \tag{157}$$

Case 4: If $\Omega = 0$ and $\sigma \neq 0$, then we have

$$q(x,t) = \pm e^{i\psi}\left(\sqrt{2}\mathrm{ia}+\frac{2\left(\mathrm{e}^{\sigma z}+\frac{\Omega}{\sigma^2}(\mathrm{e}^{\sigma z}-\rho)^2\right)}{i\left(1+\frac{1}{\sigma}(\mathrm{e}^{\sigma z}-\rho)\right)}\right), \tag{158}$$

$$p(x,t) = -a^2+\frac{2\sqrt{2}a\left(\mathrm{e}^{\sigma z}+\frac{\Omega}{\sigma^2}(\mathrm{e}^{\sigma z}-\rho)^2\right)}{1+\frac{1}{\sigma}(\mathrm{e}^{\sigma z}-\rho)}-\frac{2\left(\mathrm{e}^{\sigma z}+\frac{\Omega}{\sigma^2}(\mathrm{e}^{\sigma z}-\rho)^2\right)^2}{\left(1+\frac{1}{\sigma}(\mathrm{e}^{\sigma z}-\rho)\right)^2}, \tag{159}$$

where

$$z = d_0+\frac{\Gamma(1+\gamma)}{\eta}(x^\eta-\tau t^\eta).$$

## 8. Conclusions

In this work, we have investigated the integrable Myrzakulov-XIII (M-XIII) equation, a ferromagnet-type system characterized by dispersionless dynamics and curvature-induced interactions. Using both geometric and gauge-theoretic approaches, we establish that the M-XIII equation is gauge equivalent to the complex coupled dispersionless (CCD) system via an explicit transformation. This duality reveals the deep structural relationship between the M-XIII model and other known soliton equations.

A significant aspect of this study is the extension of the M-XIII equation to its fractional form using the reduced M-fractional derivative framework. By applying the Kudryashov method, we derive new classes of exact soliton and soliton-type solutions for the fractional version of the equation and investigate their analytical structures. These results demonstrate the effectiveness of fractional calculus in exploring generalized integrable systems.

Furthermore, we examine the geometric evolution of curves and surfaces associated with the fractional M-XIII equation and construct explicit soliton surfaces using the Sym–Tafel formula. The insights gained from this work contribute to the ongoing development of fractional soliton theory and its applications in nonlinear optics, spintronics, and geometry-driven physical models.

**Author Contributions:** Conceptualization, G.N. and K.Y.; methodology, G.B. and Z.M.; resources, A.T.; writing—original draft preparation, M.Z.; writing—review and editing, G.B. and A.T.; supervision, G.N. and K.Y.; funding acquisition, M.Z. All authors have read and agreed to the published version of the manuscript.

**Funding:** This research was funded by the Science Committee of the Ministry of Science and Higher Education of the Republic of Kazakhstan (Grant No. AP25794905).

**Data Availability Statement:** The original contributions presented in this study are included in the article. Further inquiries can be directed to the corresponding authors.

**Acknowledgments:** This research was funded by the Science Committee of the Ministry of Science and Higher Education of the Republic of Kazakhstan (Grant No. AP25794905).

**Conflicts of Interest:** The authors declare no conflicts of interest.

## References

1. Zakharov, V.E.; Shabat, A.B. Exact theory of two-dimensional self-focusing and one-dimensional self-modulation of waves in nonlinear media. *Sov. Phys. JETP* **1972**, *34*, 62–69.
2. Lakshmanan, M. The Fascinating World of the Landau-Lifshitz-Gilbert Equation: An Overview. *Phil. Trans. R. Soc. A* **2011**, *369*, 1280–1300. [CrossRef] [PubMed]
3. Myrzakulov, R.; Vijayalakshmi, S.; Nugmanova, G.; Lakshmanan, M. A (2+1)-Dimensional Integrable Spin Model: Geometrical and Gauge Equivalent Counterpart, Solitons and Localized Coherent Structures. *Phys. Lett. A* **1997**, *233*, 391–396. [CrossRef]
4. Zakharov, V.E.; Takhtadzhyan, L.A. Equivalence of the nonlinear Schrödinger equation and the equation of a Heisenberg ferromagnet. *Theor. Math. Phys.* **1979**, *38*, 17–23. [CrossRef]
5. Ablowitz, M.J.; Segur, H. *Solitons and the Inverse Scattering Transform*; SIAM Studies in Applied Mathematics; SIAM: Philadelphia, PA, USA, 1981.
6. Gautam, S.; Adhikari, S.K. Solitons in a Spin-Orbit-Coupled Spin-1 Bose-Einstein Condensate. *Braz. J. Phys.* **2021**, *51*, 297–307. [CrossRef]
7. Lakshmanan, M.; Bullough, R.K. Geometry of generalised nonlinear Schrödinger and Heisenberg ferromagnetic spin equations with linearly x-dependent coefficients. *Phys. Lett. A* **1980**, *80*, 287–292. [CrossRef]
8. Ma, L.-Y.; Shen, S.-F.; Zhu, Z.-N. Soliton solution and gauge equivalence for an integrable nonlocal complex modified Korteweg-de Vries equation. *J. Math. Phys.* **2017**, *58*, 103501. [CrossRef]
9. Mikeska, H.-J.; Steiner, M. Solitary excitations in one-dimensional magnets. *Adv. Phys.* **1991**, *40*, 191–356. [CrossRef]
10. Myrzakulov, R.; Nugmanova, G.; Syzdykova, R. Gauge Equivalence Between (2+1)-Dimensional Continuous Heisenberg Ferromagnetic Models and Nonlinear Schrödinger-Type Equations. *J. Phys. A Math. Theor.* **1998**, *31*, 9535–9545. [CrossRef]
11. Porsezian, K.; Tamizhmani, K.M.; Lakshmanan, M. Geometrical equivalence of a deformed Heisenberg spin equation and the generalized nonlinear Schrödinger equation. *Phys. Lett. A* **1987**, *124*, 159–160. [CrossRef]
12. Arnold, V.I. *Mathematical Methods of Classical Mechanics*; Springer: Berlin/Heidelberg, Germany, 1978.
13. Olver, P.J. *Applications of Lie Groups to Differential Equations*; Springer: Berlin/Heidelberg, Germany, 1993.
14. Terng, C.L.; Uhlenbeck, K. Geometry of solitons. *Not. AMS* **2000**, *47*, 17–25.
15. Sasaki, R. Soliton equations and pseudospherical surfaces. *Nucl. Phys. B* **1979**, *154*, 343–357. [CrossRef]
16. Takhtajan, L.A. Integration of the continuous Heisenberg spin chain through the inverse scattering method. *Phys. Lett. A* **1977**, *64*, 235–238. [CrossRef]
17. Matveev, V.B.; Salle, M.A. *Darboux Transformations and Solitons*; Springer: Berlin/Heidelberg, Germany, 1991.
18. Jiao, W.; Xianguo, G.; Xin, W. An integrable generalization of the Fokas–Lenells equation: Darboux transformation, reduction and explicit soliton solutions. *Chin. Phys. B* **2024**, *33*, 070202.
19. Batool, N.; Masood, W.; Siddiq, M.; Alhejaili, W.; El-Sherif, L.S.; El-Tantawy, S.A. Interaction of Gardner dust ion-acoustic multiple solitons in a dusty plasma: Insights from Cassini observations. *Braz. J. Phys.* **2025**, *55*, 112. [CrossRef]
20. Lakshmanan, M. Continuum spin system as an exactly solvable dynamical system. *Phys. Lett. A* **1977**, *61*, 53–54. [CrossRef]
21. Myrzakulov, R.; Daniel, M.; Amuda, R. Nonlinear spin-phonon excitations in an inhomogeneous compressible biquadratic Heisenberg spin chain. *Physica A* **1997**, *234*, 715–724. [CrossRef]
22. Myrzakulov, R.; Pashaev, O.; Kholmurodov, K. Particle-like excitations in many-component magnon-phonon systems. *Phys. Scr.* **1986**, *33*, 378–384. [CrossRef]
23. Yan, Z.-W.; Chen, M.-R.; Wu, K.; Zhao, W.-Z. (2+1)-Dimensional integrable Heisenberg supermagnet model. *J. Phys. Soc. Jpn.* **2012**, *81*, 094006. [CrossRef]

24. Yan, Z.-W.; Chen, M.-R.; Wu, K.; Zhao, W.-Z. Integrable deformations of the (2+1)-dimensional Heisenberg ferromagnetic model. *Commun. Theor. Phys.* **2012**, *58*, 463–468. [CrossRef]
25. Myrzakulov, R.; Lakshmanan, M.; Vijayalakshmi, S.; Danlybaeva, A. Motion of curves and surfaces and nonlinear evolution equations in (2+1) dimensions. *J. Math. Phys.* **1998**, *39*, 3765–3771.
26. Myrzakulov, R.; Makhankov, V.G.; Pashaev, O. Gauge equivalence, supersymmetry and classical solutions of the ospu(1,1/1) Heisenberg model and the nonlinear Schrödinger equation. *Lett. Math. Phys.* **1988**, *16*, 83–92.
27. Anco, S.C.; Myrzakulov, R. Integrable generalizations of Schrödinger maps and Heisenberg spin models from Hamiltonian flows of curves and surfaces. *J. Geom. Phys.* **2010**, *60*, 1576–1603. [CrossRef]
28. Myrzakulov, R.; Martina, L.; Kozhamkulov, T.A.; Myrzakul, K. Integrable Heisenberg ferromagnets and soliton geometry of curves and surfaces. In *Nonlinear Physics: Theory and Experiment. II*; World Scientific: London, UK, 2003; pp. 248–253.
29. Martina, L.; Myrzakul, K.; Myrzakulov, R.; Soliani, G. Deformation of surfaces, integrable systems, and Chern–Simons theory. *J. Math. Phys.* **2001**, *42*, 1397–1417. [CrossRef]
30. Feng, B.-F.; Maruno, K.; Ohta, Y. Geometric formulation and multi-dark soliton solution to the defocusing complex short pulse equation. *Stud. Appl. Math.* **2017**, *138*, 343–367. [CrossRef]
31. Novikov, S. The Hamiltonian formalism and a multivalued analogue of Morse theory. *Russ. Math. Surv.* **1982**, *37*, 1–56. [CrossRef]
32. Balakrishnan, R. Geometry and nonlinear evolution equations. *Pramana J. Phys.* **1997**, *48*, 189–204. [CrossRef]
33. Hussien, R.A.; Mohamed, S.G. Generated surfaces via inextensible flows of curves in $R^3$. *J. Appl. Math.* **2016**, 6178961.
34. [CrossRef] Dullin, H.R.; Gottwald, G.A.; Holm, D.D. Camassa–Holm, Korteweg–de Vries-5 and other asymptotically equivalent equations for shallow water waves. *Fluid Dyn. Res.* **2003**, *33*, 73–95. [CrossRef]
35. Barman, H.K.; Roy, R.; Mahmud, F.; Akbar, M.A.; Osman, M.S. Harmonizing wave solutions to the Fokas–Lenells model through the generalized Kudryashov method. *Optik* **2021**, *229*, 166294. [CrossRef]
36. Sulaiman, T.; Abdulkadir, T.; Yel, G.; Bulut, H. M-fractional solitons and periodic wave solutions to the Hirota–Maccari system. *Mod. Phys. Lett. B* **2019**, *33*, 1950052. [CrossRef]
37. Cinar, M.; Secer, A.; Ozisik, M.; Bayram, M. Derivation of optical solitons of dimensionless Fokas–Lenells equation with perturbation term using Sardar sub-equation method. *Opt. Quant. Electron.* **2022**, *54*, 402. [CrossRef]
38. Xie, X.-Y.; Bo, T.; Sun, W.-R.; Sun, Y.; Liu, D.-Y. Soliton collisions for a generalized variable-coefficient coupled Hirota–Maxwell–Bloch system for an erbium-doped optical fiber. *J. Mod. Opt.* **2015**, *62*, 1374–1380. [CrossRef]
39. Feng, B.-F. Complex short pulse and coupled complex short pulse equations. *Physica D* **2015**, *297*, 62–75. [CrossRef]
40. Shen, S.; Feng, B.-F.; Ohta, Y. From the real and complex coupled dispersionless equations to the real and complex short pulse equations. *Stud. Appl. Math.* **2016**, *136*, 64–88. [CrossRef]
41. Matsuno, Y. Integrable multi-component generalization of a modified short pulse equation. *J. Math. Phys.* **2016**, *57*, 111507. [CrossRef]
42. Ghosh, U.N.; Abdikian, A.; Chatterjee, P. Study of multi-solitons, breather soliton structures with (r,q) distributed ions and electrons. *Braz. J. Phys.* **2024**, *54*, 218. [CrossRef]
43. Zhassybayeva, M.; Bekova, G.; Yesmakhanova, K.; Myrzakulov, R. Integrable motions of curves of the induced Fokas–Lenells equation. *Optik* **2023**, *286*, 170979. [CrossRef]
44. Yesmakhanova, K.; Zhassybayeva, M.; Myrzakulov, R. Soliton surfaces induced by the Fokas–Lenells equation. *J. Phys. Conf. Ser.* **2019**, *1416*, 012042. [CrossRef]
45. Myrzakul, A.; Myrzakulov, R. Integrable motion of two interacting curves, spin systems and the Manakov system. *Int. J. Geom. Methods Mod. Phys.* **2016**, *13*, 1550134. [CrossRef]
46. Awadalla, M.; Taishiyeva, A.; Myrzakulov, R.; Alahmadi, J.; Zaagan, A.A.; Bekir, A. Exact analytical soliton solutions of the M-fractional Akbota equation. *Sci. Rep.* **2024**, *14*, 13360. [CrossRef]